Carbon 118 (2017) 319–326

Contents lists available at ScienceDirect

Carbon

journal homepage: www.elsevier.com/locate/carbon

Luminescence origin of carbon based dots obtained from citric acid and amino group-containing molecules

Qingqing Fang [a], Yongqiang Dong [a, *], Yingmei Chen [a], Chun-Hua Lu [a], Yuwu Chi [a], Huang-Hao Yang [a], Ting Yu [b, **]

[a] The Key Laboratory of Analysis and Detection Technology for Food Safety of the MOE and Fujian Province, State Key Laboratory of Photocatalysis on Energy and Environment College of Chemistry, Fuzhou University, Fujian 350108, China
[b] Division of Physics and Applied Physics School of Physical and Mathematical Sciences Nanyang Technological University, Singapore 637371, Singapore

ARTICLE INFO

Article history:
Received 10 October 2016
Received in revised form
9 March 2017
Accepted 17 March 2017
Available online 21 March 2017

ABSTRACT

Carbon based dots (CDs) have attracted broad attention exhibit due to the unique optical properties. However, the exact origins of their optical properties are still controversial. Citric acid (CA) coupled with some amino group-containing small molecules are believed to be ideal precursors for the synthesis of high luminescent CDs through various thermal treatment processes. Herein, CA coupled with four amino group-containing small molecules are chosen as models to synthesize CDs for a systematical study on the photoluminesce (PL) properties. It is found that the PL properties of CDs are resulted from the synergistic effect of the contained luminescent pyridine-derivatives and the defect states. A reasonable mechanism of PL emission from the CDs has been proposed. The results presented here must be critical for understanding the origins of PL, and also for preparing CDs with strong and wavelength tunable PL emission.

1. Introduction

Carbon based dots (CDs) are emerging luminescent nanomaterials, usually composed of carbon cores (either graphene nanosheets or carbon nanoparticles) and oxygen-containing functional groups [1–3]. Due to the quantum confinement and edge effect, CDs exhibit unique optical and electro-optical properties, and have accordingly attracted increasing attention [4–6]. Moreover, these CDs usually show none/low toxicity, robust optical/chemical inertness, and are easy to be obtained with low cost. Photoluminescence (PL) is the most important property, based on which CDs have been widely applied in many fields including bioimaging and sensing [3,7,8]. Substantial attention has been paid to the preparation of high photoluminescent CDs. In general, the preparation methods can be classified into "top-down" and "bottom-up" approaches, which refer to cutting big-size carbon sources and carbonizing some special organics into small-size CDs, respectively [6,9]. Although, many "top-down" methods are very facile and suitable for preparing CDs in large-scale, the PL quantum yields (PLQY) of the obtained CDs are usually low (less than 10%), partially resulted from the surface-passivation [10]. In contrast, the "bottom-up" methods seem to be much more hopeful to synthesize CDs with high PLQY [10]. Various organics, such as some carbohydrate, aromatic organics and vegetations, can be used as the precursors to prepare CDs through different "bottom-up" methods [11–14]. In particular, citric acid (CA) coupled with some amino group-containing small molecules, such as L-cysteine [15], glycine [15], ethanolamine [16], thiourea and ethylenediamine [17,18], are believed to be the most suitable precursors to synthesize high photoluminescent CDs. For example, the CDs synthesized by thermally treating the complex of CA and L-cysteine possess PLQY higher than 70% [15], and the CDs from the complex of CA and ethylenediamine show even higher PLQY, e.g. 80% [17].

Besides preparing various CDs, great efforts have been focused on understanding the PL mechanism of those CDs [19,20]. Although some hypotheses have been proposed to explain the PL behaviors of CDs, such as electronic conjugate structures and emissive traps [2,21–23]. However, it is still unclear why the CDs prepared by "bottom-up" methods, especially those from CA coupled with amino group-containing molecules, exhibit much higher PLQYs than other precursors. Recent results indicated that the extreme high PLQYs of these CDs may be related to some highly luminescent fluorophores [24–30]. Furthermore, it has been proposed that the

* Corresponding author.
** Corresponding author.
E-mail addresses: dongyq@fzu.edu.cn (Y. Dong), yuting@ntu.edu.sg (T. Yu).

http://dx.doi.org/10.1016/j.carbon.2017.03.061
0008-6223/

CDs should contain multiple PL centers, such as sp^2-hybridized core, edge states, surface functional groups. In this work, we would further investigate the relationships among the PL properties, the small fluorophore molecules and the surface states of the CDs from CA coupled with amion group-containing molecules.

It has been reported that the CDs from CA coupled with L-cysteine or ethylenediamine have extreme high PLQYs (more than 70%) [15,17], CDs from CA coupled with ethanolamine show relative high PLQY (ca. 50%) [16], and CDs from CA coupled glycine exhibite low PLQY (ca. 17%) [15]. Herein, CA coupled with the four amino group-containing small molecules (L-cysteine, ethanolamine, ethylenediamine and glycine) are chosed as model precursors to synthesize CDs (named CDs1, CDs2, CDs3 and CDs4, correspondingly). Then, the PL behaviors of the four obtained CDs are studied systematically. It is found that these CDs contain abundant high PL conjugating units (mainly some pyridine-derivatives) and a lot of carbon units with defect states (namely the C-related dangling bonds of spin $S = 1/2$). The main emission spectra of the CDs are primarily dependent on the property of the contained conjugating units, while the PLQY of the CDs is affected greatly by both the property of the contained conjugating units and the relative density of defect states. Finally, a reasonable model has been proposed to explain the PL behaviors of these CDs. These results may provide us a new insight into the PL mechanism of the CDs obtained from CA coupled with amino group-containing molecules. More importantly, inspiration may be gained from the results, to prepare high PL CDs with tunable emission spectra.

2. Experimental

2.1. Materials

Citric acid (99.9%), L-cysteine (97.0%), glycine (99.0%), ethanolamine (99.0%), ethylenediamine (99.0%), citrazinic acid (97.0%) and quinine sulfate (≥98.0%) were purchased from Sigma-Aldrich and used as received.

2.2. Preparation of CDs and control-CDs (C-CDs)

Four kinds of CDs were synthesized by thermal treating the mixture of citric acid and amino group-containing molecules. In typical preparation procedures, 1 mM CA monohydrate (2.10 g) and 0.5 mM amino group-containing molecule (0.605 g L-cysteine, 0.30 mL ethanolamine, 0.33 mL ethylenediamine or 0.375 g glycine) were dissolved in 3 mL water and heated at 70 °C for 24 h. Subsequently, the mixtures were heated hydrothermally in a Teflon-equipped stainless-steel autoclave at 220 °C for 3 h. Finally, all the four as-obtained materials were separated into two fractions (>1 kDa and <1 kDa) by dialyzing against deionized water through a dialysis bag (retained molecular weight: 1 kDa) for a week. The fractions of >1 kDa labeled as CDs1, CDs2, CDs3 and CDs4, respectively. The fractions of <1 kDa were collected and labeled as F1, F2, F3, F4, respectively. For the synthesis of C-CDs, CA only was used as the precursor, using the same method described above.

2.3. Instrumentation

The transmission electron microscopy (TEM) and high-resolution TEM (HRTEM) images were recorded on a HRTEM JEOL 2100 system operating at 200 kV. Fourier transform infrared (FTIR) spectra were obtained on a FTIR spectrophotometer (Thermo Nicolet 360). UV/Vis spectra were obtained by a UV/Vis spectrophotometer (Lambda 750). All PL spectra were obtained by a spectrophotometer (F 4600). Electrochemiluminescence (ECL) measurements are carried out by an ECL & EC multi-functional detection system (MPI-E, Remex Electronic Instrument Lt. Co., Xi'an, China) equipped with three electrodes system (a Pt wire working electrode with area of 0.31 cm^2, a Pt wire counter electrode and an Ag/AgCl reference electrode). Elemental analysis was performed on an organic elemental analyser (VarioMICRO). Electron Paramagnetic Resonance (EPR) spectra were recorded on a Bruker A-300-EPR X-band spectrometer. Mass spectra of the organics in the four filtrates are measured using an Exactive Plus mass spectrometer. The PL decays were recorded a Fluorescence Steady State and TCSPC Fluorescence Lifetime Spectro-Fluorimeter (FLS920, Edinburgh Instruments, UK). X-ray powder diffraction (XRD) pattern was obtained from a Rigaku D/max-3C (Japan) using Cu Ka radiation. Single-crystal structure analysis: Crystals were collected on a RIGAKU/SATURN 724 CCD diffractometer equipped with a fine focus, 2.0 kW sealed tube X-ray source (MoKα radiation, $\lambda = 0.71073$ Å) operating at 50 kV and 40 mA. Raman spectra were measured using a Renishaw 1000 microspectrometer (excitation wavelength of 632.8 nm). The CD samples for the Raman investigation were mixed with $CuSO_4$ to quench the PL signal. X-ray photoelectron spectroscopy (XPS) spectra of CDs were measured using an ESCAlab 250 XPS system having an Al K source.

3. Results and discussion

3.1. Structural characterization of CDs

During the dialysis processes, both of the inside and outside solutions were collected. The amount variations of the luminorphores inside and outside of the bags against dialysis time were monitored by measuring the PL intensity. It can be seen that the PL intensities of the four kinds of CDs decrease sharply in the two days, decrease slowly in the subsequent three days, then have nearly no decrease in the last two days (Fig. S1). Contrarily, the PL intensities of the four filtrates increase dramatically in the first two days, and increase slowly in the following three days, then have nearly no increase in the last two days. The results indicate that the dialysis is completed within one week.

The TEM images (Fig. 1) reveal that the lateral size of the obtained four CDs is 4–8 nm. The HRTEM images indicate that all the CDs are crystalline with lattice spacing of about 0.24 nm, which corresponds to the in-plane lattice spacing of graphite (100). The morphologies of all the CDs have no obvious difference from that of C-CDs from the hydrothermal treatment of CA only (Fig. S2). The Raman spectra (Fig. S3) of all the four CDs show the characteristic "disorder" D and crystalline G bands at around 1385 and 1580 cm^{-1}, respectively. The FTIR spectra of CDs (Fig. S4) exhibit the absorption peaks of C=C groups at around 1650 cm^{-1}, the peaks of C=O group at around 1710 cm^{-1}, the peaks of COO^- groups at 1550 and 1420 cm^{-1}, and the peaks of C–O, C–N and/or C–S groups at around 1185 cm^{-1}. The XPS spectra (Fig. S5) further confirm the results from the FTIR. Furthermore, the high resolution XPS spectra of N1s indicate that the nitrogen atoms in the CDs are presented mainly in the form of pyridinic type. The results indicate that all the four CDs have similar structural characterizations of most commonly reported CDs, namely a carbon core of graphite nature and a surface with functional groups [3]. The XRD patterns of the four CDs show a broad peak centered at around 21.0° (Fig. S6), which is smaller than that of graphite. It suggests that the interlayer distances of the CDs are larger than that of graphite due to the presence of the functional groups.

3.2. Optical characterization of CDs

As shown in Fig. 2a–d, all the four obtained CDs present strong PL activities, i.e. they show bright blue emission under the

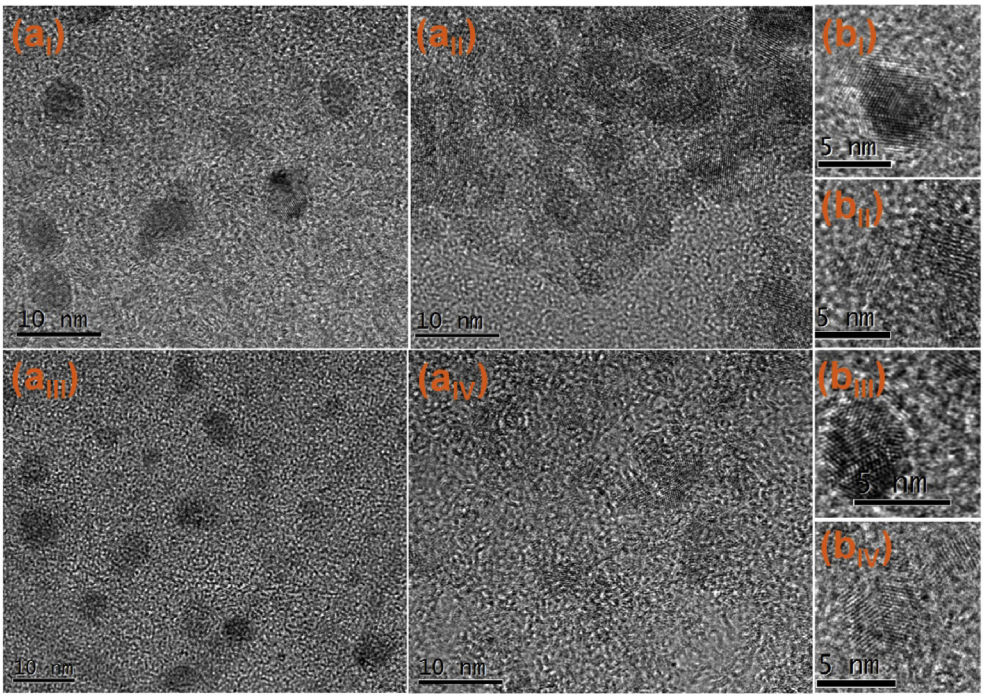

Fig. 1. TEM and HRTEM images of CDs1 (a_I, b_I), CDs2 (a_{II}, b_{II}), CDs3 (a_{III}, b_{III}), and CDs4 (a_{IV}, b_{IV}). (A colour version of this figure can be viewed online.)

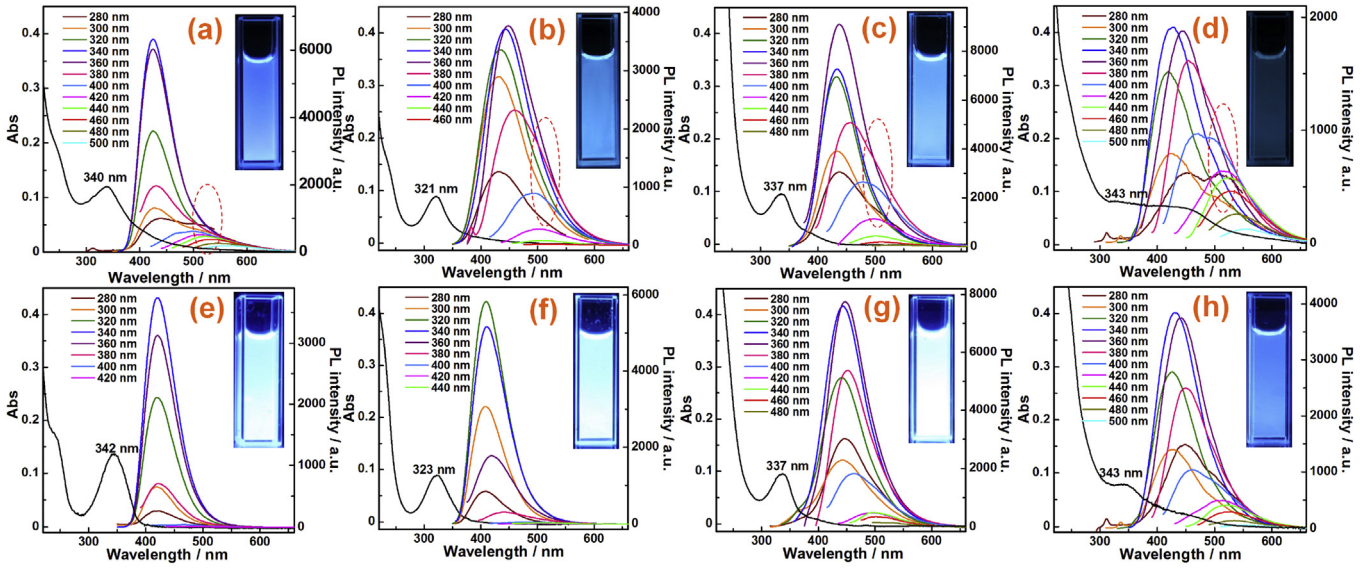

Fig. 2. UV–vis and PL spectra of CDs1 (a), CDs2 (b), CDs3 (c), CDs4 (d), F1 (e), F2 (f), F3 (g), F4 (h). The insets show the corresponding PL images under the excitation of 365 nm UV light. (A colour version of this figure can be viewed online.)

illumination of 365 nm UV light. The PL spectra indicate that the emission wavelengths of all the four CDs are dependent on the excitation wavelengths, red-shifting with the gradual increase of excitation wavelengths. All of the four CDs show a main PL peak at around 420–440 nm and a PL shoulder at around 525 nm, and exhibit a broad UV–vis absorption band with a peak at 320–345 nm. In general, the optical properties of the four CDs are rather similar to each other, implying some intrinsic relationship among these CDs. However, the optical properties of the four CDs are not always the same. First of all, the effects of excitation wavelength on the emission wavelength of the four CDs are different (e.g. the excitation-dependent PL behaviors of CDs1 are much slighter than those of the other three CDs). Second, the four CDs have quite different PLQY values (e.g. the PLQY of CDs1 is higher than those of the other three CDs, Table 1). Obviously, the

Table 1
The maximum excitation wavelength of the CDs and filtrates, and the PLQY of the eight fractions excited at the corresponding maximum excitation wavelength.

Fraction	CDs1	F1	CDs2	F2	CDs3	F3	CDs4	F4
EX (nm)	345	345	323	323	337	337	343	343
PLQY (%)	12.5	70.5	8.5	41.9	11.8	60.2	2.2	16

four CDs exhibit both similar and different PL properties, which would be a key clue to study the PL mechanism of these CDs, which is of significance for preparing high PL CDs.

It can be found from Table 1, although the CDs exhibit good PL behaviors, the PLQYs are not as high as those in the reported works [15–17]. It should be pointed out that most of the reported extreme high PL CDs are obtained directly from the thermal treatment without any separation or purification, while the four CDs here are finally obtained after a long-term dialysis against deionized water through a dialysis bag. It is supposed that some high PL fractions may be contained in the filtrates (the four filtrates corresponding to the four CDs are labeled as F1, F2, F3 and F4, respectively). Therefore, the optical properties of all the four filtrates were investigated subsequently. As shown in Fig. 2e–h and Fig. S7, all the four filtrates show bright blue emission under the excitation of 365 nm UV light. The main PL bands and absorption peaks of all the filtrates agree well with those of the corresponding CDs. However, compared with the CDs, the effects of excitation wavelength on the emission spectra of the filtrates are much slighter, and the absorption peaks at 320–345 nm are sharper. More importantly, the PLQYs of the four filtrates are much higher than their corresponding CDs (see Table 1), which are quite close to the values in the reported works [15,16]. Apparently, some high PL fractions are indeed contained in the filtrates. However, only few CDs are detected by TEM in all of the four filtrates (As shown in Fig. S8, The morphologies of the CDs in the filtrates are similar with those of the corresponding CD samples. It seems that some CDs particles were leaked out from the dialysis bag mouth). This means that the PL behaviors of the four filtrates may be related to something else rather than CDs. It has been reported that the mixture of CA and ammonia water can be used to synthesize citrazinic acid [31], which shows bright blue PL. The main PL bands and the main UV absorption peaks of the four CDs are quite similar to those of citrazinic acid (see Fig. S9). As the four CDs are synthesized by hydrothermally treating the mixtures of CA and amino group-containing molecules, it is possible that similar pyridine-derivatives have been produced. The mass spectra indicate that all the four filtrates contain abundant of small molecules (Fig. 3). The organics contained in F2, F3 and F4 are relative complex, and are difficult to be separated from each other. Fortunately, the component in F1 seems quite pure. As F1 was concentrated and set quietly for a day, yellow crystals could be obtained. It has been reported that the reaction of CA and L-cys could produce a high luminescent 3,5-dihydro-5-oxo-2*H*-thiazolo [3,2-*a*]pyridine-3,7-dicarboxylic acid (TPA), whose molecular mass agreed well with the result from mass spectrum [25,27]. To prove it, the crystals were characterized by X-ray single-crystal diffraction (Table S1, S2, Fig. S10), elemental analysis (Table S3) and XRD (Fig. S11). The results confirm that the crystals are TPA.

The optical properties of TPA were investigated (see Fig. S12). As expected, the optical behaviors including UV–vis absorption and PL spectra agree well with those of F1. The PLQY is calculated to be 90.5%, which is higher than that of F1. These results indicate that the PL of F1 should be mainly originated from the contained TPA. Combing the mass spectra (Fig. 3) and the structural formulas of the amino group-containing molecules used in preparing the other three CDs, some structural formulas can be proposed for the organics contained in the other filtrates (Fig. 3). Many of these organics are pyridine-derivatives with similar conjugating structures with units of citrazinic acid or TPA. Apparently, the PL properties of the other 3 filtrates should be also related to these pyridine-derivatives.

3.3. Luminescence mechanisms of CDs

Herein, it can be found that hydrothermally treating the mixtures of CA and amino group-containing molecules produce not only CDs but also some high PL pyridine-derivatives, which agree well with the results of Kasprzyk's group [25]. However, some questions are still unclear. First of all, what is the relationship between the CDs and the PL pyridine-derivatives? Second, why do the CDs exhibit excitation-dependent PL emission? Third, why do the four CDs show different PL behaviors and PLQYs? In particular, why CDs4 show such a low PLQY. Therefore, it is necessary to investigate and discuss the PL mechanism of CDs to answer these questions.

Although the exact PL mechanisms of CDs are still an open question, a large quantity evidences indicate that the PL behaviors of CDs are mainly related to the localized conjugating structural units and defect states [1,2,22,23]. For all the four kinds of CDs, three kinds of conjugating units may be contained. Firstly, all the CDs show a characteristic UV–vis absorption peak at around 320–345 nm and a main PL emission peak at around 420–440 nm (Fig. 2). Some research groups have proposed that the absorption peak at around 320–345 nm of this kind of CDs may be originated from the n-π^* edge transitions. Accordingly, they identified the n-π^* as a main transition in these CDs to produce edge emission [30]. However, the calculation results indicate that the absorption peak at around 320–345 nm should be mainly attributed to the π-π^* transition of the corresponding pyridine-derivatives (Fig. S13). Furthermore, the PL peaks of the CDs at around 420–440 nm also agree well with those of the corresponding pyridine-derivatives. For example, the UV–vis absorption peak and PL peak of the CDs1 fit well with those of TPA. To further prove it, a series of CDs1 were synthesized using CA coupled with different ratio of L-cysteine. It is found that the absorption peak intensity at around 343 nm of the as-obtained CDs1 increases as the amount of L-cysteine increasing from 0.01 to 0.2 g (Fig. S14). Correspondingly, the PLQY of the CDs increases from 2.6% to 12.5% (Table S4). Apparently, there are positive correlations between the PLQY of the obtained CDs1 and the amount connected TPA units. However, when the amount of CA was further increased, neither the absorption peak intensity at around 343 nm nor the PLQY of the obtained CDs enhance, indicating that the TPA units connected on the CDs1 have reached the maximum. Apparently, the pyridine-derivatives play important roles on the optical properties of the CDs. It has been mentioned above that all the CDs are obtained after a long time dialysis, the pyridine-derivatives should not be present freely in these CD samples. However, all the CDs and pyridine-derivatives have a lot of oxygen-containing functional groups, such as hydroxyl and carboxyl groups. In the hydrothermal treatment, some pyridine-derivative molecules may be connected covalently on the CDs due to the condensation reactions among the functional groups. Then, the connected pyridine-derivative molecules act as the isolated conjugating units to provide the CDs new energy levels. Due to the fact that the pyridine-derivative molecules are connected with CDs1 via the functional groups, the conjugation structures of pyridine-derivatives connected on the CDs have no obvious change. Therefore, the main UV–vis absorption peaks of the CDs agree well with the calculated energy gap between the highest occupied molecular orbital (HOMO) and the lowest unoccupied molecular orbital (LUMO) of the corresponding pyridine-derivatives (π-π^* transition). And the main PL emission peaks at around 420–440 nm should be mainly attributed to the connected pyridine-derivatives. The phenomenon is same as the "surface-attachment" proposed by other groups [29]. Secondly, in addition to the pyridine-derivatives, other isolated sp^2 clusters should be formed and connected on the CDs. As shown in Fig. S15, the UV–vis absorption spectrum of the C-CDs from CA only presents a small shoulder at around 300 nm. Furthermore, the C-CDs also exhibit blue PL emission. When the excitation wavelength is increased from 300 to 500 nm, the PL intensity of the C-CDs

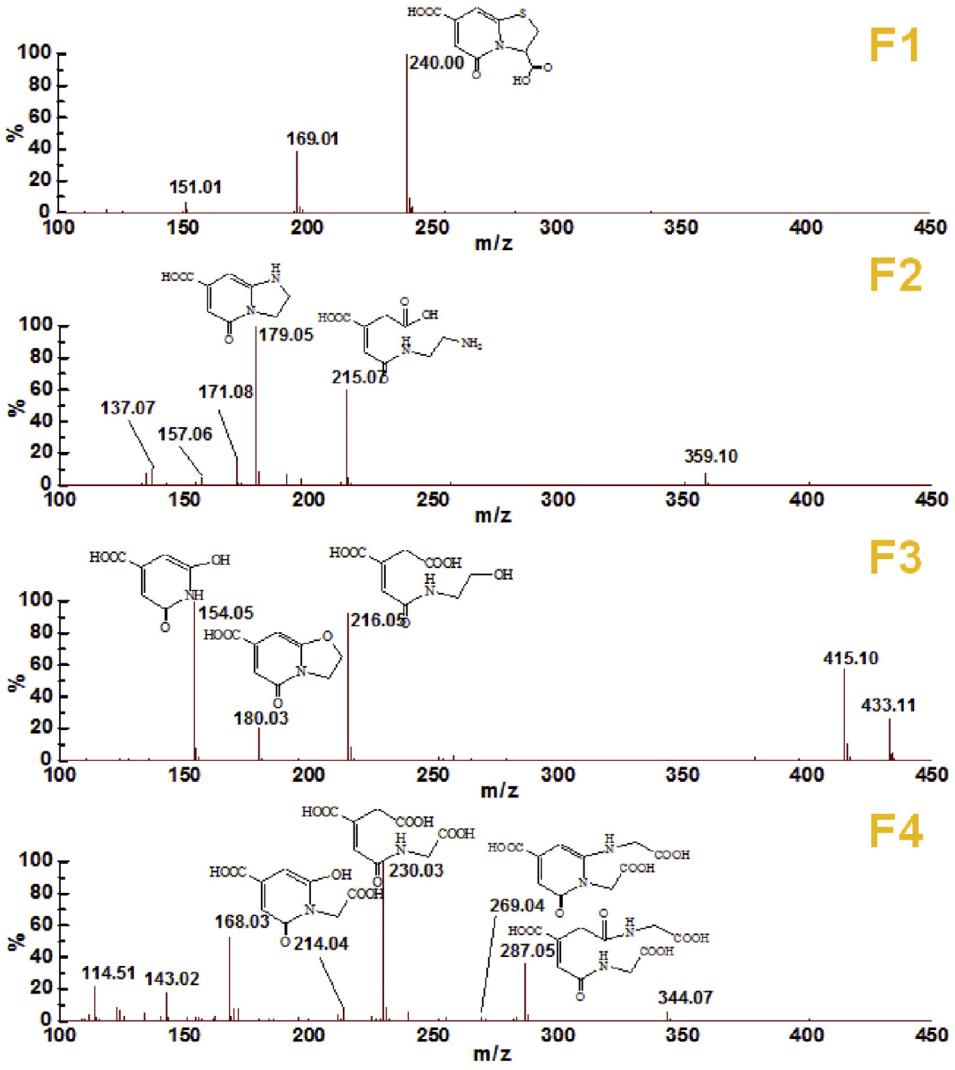

Fig. 3. Mass spectra of the main organics in the four filtrates. The insets show the structural formulas of the main organics. (A colour version of this figure can be viewed online.)

decreases gradually, accompanying with obvious red-shift of emission spectrum. The results confirm that the carbonization of CA can also produce some luminescent isolated sp^2 clusters. The UV–vis and PL spectra of the C-CDs suggest that the energy gaps between HOMO and LUMO of the isolated sp^2 clusters should be close to those of the connected pyridine-derivatives. Therefore, it is difficult to distinguish the PL emission of the isolated sp^2 clusters from the PL spectra. However, the PLQY of the C-CDs at 345 nm is calculated to be only about 1.0%, which is much lower than those of the CDs. Therefore, the pyridine-derivatives should play more important roles than the isolated sp^2 clusters on the PL properties of CDs1. Thirdly, as shown in the TEM image, CDs1 have graphitic and crystalline cores of about 5 nm lateral sizes. It has been proposed that the calculated gap between HOMO and LUMO of a cluster of 20 aromatic rings is as low as ~2 eV. The aromatic ring number contained in the crystalline cores of about 5 nm lateral size is calculated to be more than 500. Therefore, the energy gaps between the HOMO and LUMO of the crystalline cores should be much lower than 2 eV, and would have no attribution for the PL emission of CDs1 at visible wavelength range. However, crystalline cores may act as the energy acceptor, and inhibit the PL activities of CDs1 due to the fluorescence resonance energy transfer (FRET) [32].

Besides the isolated conjugating units, all the CDs have large quantities of defect states. All the four CDs exhibit one symmetric EPR signal, with corresponding zero-crossing g value of 2.003 (Fig. S16). On the contrary, the four filtrates produce nearly no EPR signal, only F4 shows a very weak EPR signal (Fig. S17). These results indicate that all the four CDs contain a large quantity of C-related dangling bonds of spin $S = 1/2$, which agree well with that of graphene nanoribbons [33–35]. The defect states also contribute to the PL behaviors of the CDs. As well known, ECL is a powerful technique to investigate the defect states of nanomaterials [36–38]. Like most CDs [39,40], all the four CDs can produce strong cathodic ECL signal in the presence of $S_2O_8^{2-}$ (Fig. S18) due to the electron-transfer between the negatively charged CDs and electro-generated $SO_4^{\cdot-}$ radicals. Thus, the ECL spectrum of the CDs can be measured in the presence of $S_2O_8^{2-}$ (Fig. 4). It can be seen that all of the four ECL spectra show a maximum at around 525 nm, which is consistent with the wavelength of the small PL peak (Fig. 2a–d). The results imply that both the ECL and PL emissions can be assigned to the same emission centers. It has been proposed that the ECL spectrum of CDs reflects the defect state energy levels of CDs [40,41]. Therefore, it can be concluded that the PL emission at around 525 nm of the CDs should be resulted from the defect states.

The experimental results mentioned above indicate that the optical properties of the four CDs should be mainly attributed to the

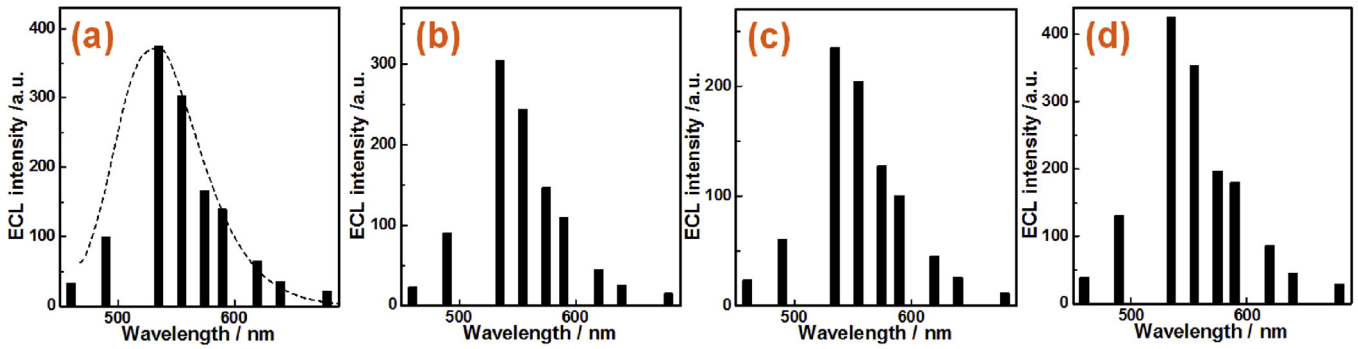

Fig. 4. ECL spectrum of the CDs1 (a) CDs2 (b), CDs3 (c), CDs4 (d) in the presence of $S_2O_8^{2}$ in 0.1 M PBS (pH 7) containing 1 M KNO_3. The concentrations of CDs are 200 μg/mL. The concentrations of $S_2O_8^{2-}$ and KNO_3 are 10 mM and 1 M, respectively. (A colour version of this figure can be viewed online.)

isolated sp^2 domains (mainly the pyridine-derivative molecules) and defect states. To further reveal the relationships between the pyridine-derivatives and the defect states, CDs1 are chosen as a model for the further investigation and discussion based on the fact that the pyridine-derivative formed in CDs1 has been confirmed. As shown in Fig. 5, the PL lifetime of the CDs1 measured at 420 nm (mainly the intrinsic emission) is measured to be 7.29 ± 0.01 ns, which much shorter than that of free TPA (9.31 ± 0.01 ns). The lifetime of the CDs1 measured at 525 nm (mainly the defect emission) is even shorter, only 5.71 ± 0.04 ns. The results suggest that the π^*-π transition of the TPA units in the CDs1 should not be an independent process. Instead, it should be affected by the defect states, leading to the decrease in PL lifetime. In brief, the optical properties of the CDs should be synergy effects from the isolated pyridine-derivative molecules and defect states. The results agree well with those of Fu's group.

Based on the discussion mentioned above, a mechanism model is proposed for the PL of the CDs. As shown in Fig. 6, CDs1 contain large quantities of conjugating units with PL (connected pyridine-derivatives and some isolated sp^2 clusters), graphitic cores and abundant defect states (C-related dandling bonds). Under the irradiation of UV light in the range from 280 to 380 nm, the electrons in the π orbitals of the luminescent conjugation units can be excited to the π^* orbitals (Process a). Then some of the excited electrons in the π^* orbitals may recombine with the holes in the π orbitals directly, emitting the PL signal centered at 420–440 nm, which can be referred as the intrinsic emission like the band-edge emission observed in QDs (Process b) [40]. However, the other excited electrons in the π orbitals may be trapped by the defect states of energies lower than in the π^* orbitals (Process c) before they are finally recombine with the holes in the π orbitals. Meanwhile, some electrons may be excited and trapped directly by the defect states (Process d). Then, the electrons trapped by the defect states (Process c, d) relax through either radiative (Process e) or nonradiative (Process f) ways. The PL signal from the radiative relaxation is the defect emission, which is also observed in QDs [42]. Therefore, when the excitation wavelength is in the range of 280–380 nm, the CDs1 produce both intrinsic PL and defect PL signal. When the excitation wavelength is longer than 380 nm, the energy of which is less than that needed for the π-π^* transition, the electrons can only be excited to the defect states. Accordingly, only the defect emission can be observed. It should be mentioned that both the intrinsic emission and defect emission of the CDs would be partially quenched by the graphitic cores due to the FRET effect. Due to the effects of the defect states and the graphitic cores, the PLQYs of the CDs are usually much lower than those of the corresponding pyridine-derivatives.

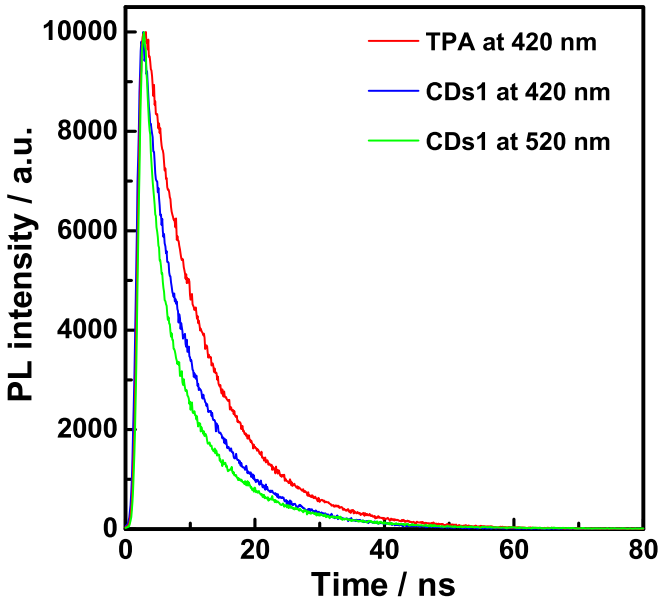

Fig. 5. PL decays (345 nm laser excitation, and monitored through 420 nm or 525 nm bandpass filters) of free TPA and CDs1. The PL decay curves fitted to a one-exponential function: $y = A_1{}^*\exp(-x/t_1) + y_0$. (A colour version of this figure can be viewed online.)

According to the built PL mechanism model, the three questions proposed above can be answered. First, the pyridine-derivatives are covalently connected on the CDs, acting as the luminescent center to produce the intrinsic PL signal. Therefore, the main PL properties of the CDs are similar with the corresponding pyridine-derivatives. Secondly, all the CDs exhibit intrinsic PL and defect emission. The excitation-dependent PL emission mainly reflects different emissive sites. Thirdly, the PLQY of the CDs mainly depends on the amount and PL properties of the contained pyridine-derivatives and the amount of defect. In other words, the different PLQYs of the four CD samples should be a synergistic effect from the factors. For example, the UV–vis spectrum of CDs4 shows only a very weak peak at around 343 nm, implying that the amount of pyridine-derivatives contained in CDs4 is low. Furthermore, the relative low PLQY of the F4 implies that the pyridine-derivative in CDs4 should have low PLQYs. Compared with the other three CD samples, the CDs4 indeed exhibit a quite low PLQY.

Thus, it can be concluded out that the main emission spectra of the CDs are mainly dependent on the nature of the connected conjugating units (pyridine-derivatives here) while the PLQYs are affect by the nature of the conjugating units and the defect states. It implies that CDs of different PL colors can be synthesized by adding

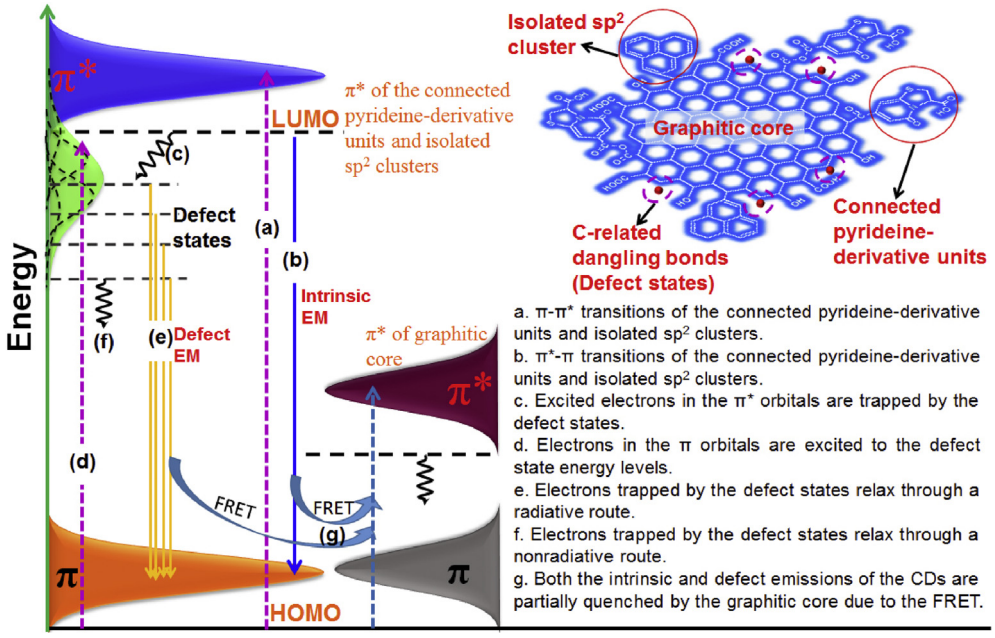

Fig. 6. Representation of the PL mechanism of CDs. (A colour version of this figure can be viewed online.)

different organics as the isolated conjugating units. Furthermore, the PLQYs of CDs can be improved by passivating the defect states.

4. Summary

CA and four amino group-containing molecules were used as the precursors to prepare four kinds of CDs. It is found that the hydrothermal treatment of these precursors produces not only CDs but also some luminescent pyridine-derivatives. The CDs contained large quantities of luminescent pyridine-derivatives and a lot of defect states, leading to the unique PL properties of CDs. A reasonable PL mechanism has been proposed for the CDs. The results imply that the main emission spectra of the CDs are dependent on the nature of the isolated conjugating units, while the PLQYs of the CDs are affected by both the nature of the isolated conjugating units and defect states. The results are quite significant for understanding the PL of CDs, and also for preparing high PL CDs with tunable emission spectra.

Acknowledgments

This study was financially supported by National Natural Science Foundation of China (21675026, 21675027), and the Program for Changjiang Scholars and Innovative Research Team in University (No. IRT1116). The authors thank Professor Xinqi Zhang at Instrumentation Analysis and Measurement Center of Fuzhou University for the help in TEM, and thank Professor Haohong Li for the help in calculation.

Appendix A. Supplementary data

Supplementary data related to this article can be found at http://dx.doi.org/10.1016/j.carbon.2017.03.061.

References

[1] Y.-P. Sun, B. Zhou, Y. Lin, W. Wang, K.S. Fernando, P. Pathak, et al., Quantum-sized carbon dots for bright and colorful photoluminescence, J. Am. Chem. Soc. 128 (24) (2006) 7756–7757.
[2] D. Pan, J. Zhang, Z. Li, M. Wu, Hydrothermal route for cutting graphene sheets into blue-luminescent graphene quantum dots, Adv. Mater 22 (6) (2010) 734–738.
[3] Y. Dong, J. Cai, X. You, Y. Chi, Sensing applications of luminescent carbon based dots, Analyst 140 (22) (2015) 7468–7486.
[4] C. Li, M.J. Meziani, S. Sahu, Y.-P. Sun, Photoluminescence properties of graphene versus other carbon nanomaterials, Acc. Chem. Res. 46 (1) (2012) 171–180.
[5] Z. Zhang, J. Zhang, N. Chen, L. Qu, Graphene quantum dots: an emerging material for energy-related applications and beyond, Energy Environ. Sci. 5 (10) (2012) 8869–8890.
[6] L. Li, G. Wu, G. Yang, J. Peng, J. Zhao, J.J. Zhu, Focusing on luminescent graphene quantum dots: current status and future perspectives, Nanoscale 5 (10) (2013) 4015–4039.
[7] J. Peng, W. Gao, B.K. Gupta, Z. Liu, R. Romero-Aburto, L. Ge, et al., Graphene quantum dots derived from carbon fibers, Nano Lett. 12 (2) (2012) 844–849.
[8] P. Huang, J. Lin, X. Wang, Z. Wang, C. Zhang, M. He, et al., Light-triggered theranostics based on photosensitizer-conjugated carbon dots for simultaneous enhanced-fluorescence imaging and photodynamic therapy, Adv. Mater 24 (37) (2012) 5104–5110.
[9] H. Li, Z. Kang, Y. Liu, S.-T. Lee, Carbon nanodots: synthesis, properties and applications, J. Mater Chem. 22 (46) (2012) 24230–24253.
[10] K. Hola, Y. Zhang, Y. Wang, E.P. Giannelis, R. Zboril, A.L. Rogach, Carbon dots—emerging light emitters for bioimaging, cancer therapy and optoelectronics, Nano Today 9 (5) (2014) 590–603.
[11] R. Liu, D. Wu, X. Feng, K. Mullen, Bottom-up fabrication of photoluminescent graphene quantum dots with uniform morphology, J. Am. Chem. Soc. 133 (39) (2011) 15221–15223.
[12] X. Teng, C. Ma, C. Ge, M. Yan, J. Yang, Y. Zhang, et al., Green synthesis of nitrogen-doped carbon dots from konjac flour with "off–on" fluorescence by Fe^{3+} and l-lysine for bioimaging, J. Mater Chem. B 2 (29) (2014) 4631–4639.
[13] J. Zhang, W. Shen, D. Pan, Z. Zhang, Y. Fang, M. Wu, Controlled synthesis of green and blue luminescent carbon nanoparticles with high yields by the carbonization of sucrose, New J. Chem. 34 (4) (2010) 591–593.
[14] X. Yan, X. Cui, L.-S. Li, Synthesis of large, stable colloidal graphene quantum dots with tunable size, J. Am. Chem. Soc. 132 (17) (2010) 5944–5945.
[15] Y. Dong, H. Pang, H.B. Yang, C. Guo, J. Shao, Y. Chi, et al., Carbon-based dots co-doped with nitrogen and sulfur for high quantum yield and excitation-independent emission, Angew. Chem. Int. Ed. 52 (30) (2013) 7800–7804.
[16] M.J. Krysmann, A. Kelarakis, P. Dallas, E.P. Giannelis, Formation mechanism of carbogenic nanoparticles with dual photoluminescence emission, J. Am. Chem. Soc. 134 (2) (2012) 747–750.
[17] S. Zhu, Q. Meng, L. Wang, J. Zhang, Y. Song, H. Jin, et al., Highly photoluminescent carbon dots for multicolor patterning, sensors, and bioimaging, Angew. Chem. Int. Ed. 52 (14) (2013) 3953–3957.
[18] D. Qu, M. Zheng, P. Du, Y. Zhou, L. Zhang, D. Li, et al., Highly luminescent S, N co-doped graphene quantum dots with broad visible absorption bands for visible light photocatalysts, Nanoscale 5 (24) (2013) 12272–12277.
[19] Y. Park, J. Joo, B. Lim, W. Kwon, S.-W. Rhee, Improving the functionality of carbon nanodots: doping and surface functionalization, J. Mater Mater A 4

(30) (2016) 11582–11603.
[20] J. Schneider, C.J. Reckmeier, Y. Xiong, M. Seckendorff, A.S. Susha, P. Kasák, et al., Molecular fluorescence in citric acid-based carbon dots, J. Phys. Chem. C 121 (3) (2017) 2014–2022.
[21] J. Zhou, C. Booker, R. Li, X. Zhou, T.-K. Sham, X. Sun, et al., An electrochemical avenue to blue luminescent nanocrystals from multiwalled carbon nanotubes (MWCNTs), J. Am. Chem. Soc. 129 (4)) (2007) 744–745.
[22] Y. Dong, J. Shao, C. Chen, H. Li, R. Wang, Y. Chi, et al., Blue luminescent graphene quantum dots and graphene oxide prepared by tuning the carbonization degree of citric acid, Carbon 50 (12) (2012) 4738–4743.
[23] K.P. Loh, Q. Bao, G. Eda, M. Chhowalla, Graphene oxide as a chemically tunable platform for optical applications, Nat. Chem. 2 (12) (2010) 1015–1024.
[24] S. Zhu, X. Zhao, Y. Song, S. Lu, B. Yang, Beyond bottom-up carbon nanodots: citric-acid derived organic molecules, Nano Today 11 (2) (2016) 128–132.
[25] W. Kasprzyk, S. Bednarz, D. Bogdal, Luminescence phenomena of biodegradable photoluminescent poly(diol citrates), Chem. Comm. 49 (57) (2013) 6445–6447.
[26] M. Fu, F. Ehrat, Y. Wang, K.-Z. Milowska, C. Reckmeier, A.-L. Rogach, et al., Carbon dots: a unique fluorescent cocktail of polycyclic aromatic hydrocarbons, Nano Lett. 15 (9) (2015) 6030–6035.
[27] W. Kasprzyk, S. Bednarz, P. Żmudzki, M. Galica, D. Bogdał, Novel efficient fluorophores synthesized from citric acid, RSC Adv. 5 (44) (2015) 34795–34799.
[28] Y. Song, S. Zhu, S. Zhang, Y. Fu, L. Wang, X. Zhao, et al., Investigation from chemical structure to photoluminescent mechanism: a type of carbon dots from the pyrolysis of citric acid and an amine, J. Mater Chem. C 3 (23) (2015) 5976–5984.
[29] C.-J. Reckmeier, J. Schneider, A.-S. Susha, A.-L. Rogach, Luminescent colloidal carbon dots: optical properties and effects of doping [Invited], Opt. Express 24 (2) (2016) A312–A340.
[30] C.-J. Reckmeier, Y. Wang, R. Zboril, A.-L. Rogach, Influence of doping and temperature on solvatochromic shifts in optical spectra of carbon dots, J. Phys. Chem. C 120 (19) (2016) 10591–10604.
[31] S. Ruhemann, XLI.—Formation of pyridine-derivatives from citric acid, and on the constitution of pyridine, J Chem Soc Trans 51 (1887) 403–409.
[32] H. Li, J. Zhai, J. Tian, Y. Luo, X. Sun, Carbon nanoparticle for highly sensitive and selective fluorescent detection of mercury(II) ion in aqueous solution, Biosens. Bioelectron. 26 (12) (2011) 4656–4660.
[33] Y. Dong, L. Wan, J. Cai, Q. Fang, Y. Chi, G. Chen, Natural carbon-based dots from humic substances, Sci. Rep. 5 (2015) 10037.
[34] C. Su, M. Acik, K. Takai, J. Lu, S.-J. Hao, Y. Zheng, et al., Probing the catalytic activity of porous graphene oxide and the origin of this behaviour, Nat. Commun. 3 (2012) 1298.
[35] A. Thess, R. Lee, P. Nikolaev, H. Dai, P. Petit, J. Robert, Crystalline ropes of metallic carbon nanotubes, Science 273 (5274) (1996) 483–487.
[36] Y. Bae, N. Myung, A.J. Bard, Electrochemistry and electrogenerated chemiluminescence of CdTe nanoparticles, Nano Lett. 4 (6) (2004) 1153–1161.
[37] S.K. Poznyak, D.V. Talapin, E.V. Shevchenko, H. Weller, Quantum dot chemiluminescence, Nano Lett. 4 (4) (2004) 693–698.
[38] Z. Ding, B.M. Quinn, S.K. Haram, L.E. Pell, B.A. Korgel, A.J. Bard, Electrochemistry and electrogenerated chemiluminescence from silicon nanocrystal quantum dots, Science 296 (5571) (2002) 1293–1297.
[39] Y. Dong, N. Zhou, X. Lin, J. Lin, Y. Chi, G. Chen, Extraction of electrochemiluminescent oxidized carbon quantum dots from activated carbon, Chem. Mater 22 (21) (2010) 5895–5899.
[40] L.-L. Li, J. Ji, R. Fei, C.-Z. Wang, Q. Lu, J.-R. Zhang, et al., A facile microwave avenue to electrochemiluminescent two-color graphene quantum dots, Adv. Funct. Mater 22 (14) (2012) 2971–2979.
[41] L. Zheng, Y. Chi, Y. Dong, J. Lin, B. Wang, Electrochemiluminescence of water-soluble carbon nanocrystals released electrochemically from graphite, J. Am. Chem. Soc. 131 (13) (2009) 4564–4565.
[42] D. Bera, L. Qian, T.-K. Tseng, P.H. Holloway, Quantum dots and their multimodal applications: a review, Materials 3 (4) (2010) 2260–2345.